Hydrothermal Synthesis and Characterization of Hybrid ZnO/3D Graphene Structures

ELENA CHITANU, CRISTINA BANCIU*, GABRIELA SBARCEA, VIRGIL MARINESCU, ADELA BARA, PAULA BARBU (PRIOTEASA)
National Institute for Research and Development in Electrical Engineering ICPE-CA, 313 Splaiul Unirii, 030138, Bucharest, Romania

In this paper we obtained hybrid ZnO/3D graphene structures through hydrothermal growth of ZnO nanoparticles on 3D graphene substrate obtained by chemical vapour deposition (CVD) method in order to use them as electrode in solar cells. The influence of hydrothermal process parameters on structural and morphological properties of the obtained ZnO nanoparticles was studied. The temperature and the duration of the process had an important influence on the ZnO nanostructures obtaining.

Keywords: 3D graphene, hybrid structures, zinc oxide, hydrothermal synthesis

In the last years, due to the increasing interest for hybrid structures that combine materials with different properties it was necessary to synthesize novel materials that combine one-dimensional (1D) and two-dimensional (2D) components. From the carbon family, graphene has been the most attractive material in the last years [1, 2], due to its monolayer structures with sp^2 hybrid carbon atoms. A hybrid structure with improved properties and especially with a high chemical stability was obtained by growing 1D zinc oxide (ZnO) nanoparticles on 2D graphene structures [1].

Recently, we can notice the emergence of three-dimensional graphene as a new class of multifunctional materials, which have a variety of potential applications, ranging from energy storage to bioelectronics [3-5]. Their multifunctional nature stems from a unique combination of mechanical properties, electrical conductivity, ultra-low density and high specific surface areas, which makes them different from any other polymer, ceramic or metal material [6]. As opposed to the chemical route for producing reduced graphene oxide (rGO) sheets, the CVD method leads to the production of high-quality graphene, which displays fewer structural defects [7].

Carbon nanomaterials like fullerenes, carbon nanotubes (CNTs) and graphene are currently being intensively investigated in solar cell applications due to their unique electrical properties, large specific surface area, and extraordinary chemical and mechanical stability [8, 9]. Incorporation of the carbon nanomaterials into the matrix of the photoanode enables the improvement of the performance of absorbing layers by enhancing the light absorption and electron transport in the semiconducting nanostructured film [10, 11]. Incorporating CNTs into ZnO electrodes provided highly conductive paths to the ZnO nanostructures, thereby promoting faster transport of photoinduced electrons in dye-sensitized solar cells (DSSCs) and therefore higher current [12, 13].

To prepare high-quality 1D ZnO nanoparticles several methods have been developed such as hydrothermal growth [14], vacuum thermal evaporation [15], metal-organic chemical vapour deposition [16], vapour phase epitaxial [17], vapour phase transport [18] and vapour-liquid-solid method [19]. The advantages of the hydrothermal method [20] over the methods mentioned previously are the following: (1) cheaper cost of this process because it doesn’t need special equipment, and (2) uniform nanoparticles can be obtained on complex geometry of the substrate.

ZnO nanostructures are promising materials in optics, optoelectronics, sensors, supercapacitors, and actuators due to their semiconducting, piezoelectronic, and pyroelectric properties [21-24]. Nanostructured ZnO possesses high specific surface area, biocompatibility and excellent electrochemical activity, making it desirable for high performance supercapacitors and biosensors [25]. Due to these unique properties ZnO has been used widely for the fabrication of DSSC photoanodes. ZnO is regarded as an attractive alternative to titanium dioxide (TiO_2) because it has a similar band gap level to that of TiO_2 while possesses a higher electron mobility and more flexibility in synthesis and morphologies [26, 27].

A hybrid structure with improved properties and especially with a high chemical stability was obtained very recently by using zinc oxide nanosheets and 3D graphene structures [28, 29]. This hybrid ZnO/graphene structure with special properties for solar cells, especially DSSC type, has been synthesized by combining the two materials with complementary properties, namely graphene with the ability to accept electrons and ZnO with an intensive catalytic activity. A DSSC was fabricated by electro-deposition process using a graphene layer/ZnO nanosheets as nanocomposite film [28].

In this paper, a hybrid ZnO/3D graphene structure was successfully obtained by growing 1D ZnO nanoparticles on a 3D graphene substrate using hydrothermal synthesis. The influence of the hydrothermal process parameters (like temperature and time) on the properties of the hybrid 3D structure was studied by structural and morphological characterization.

Experimental part

The 3D graphene was obtained by CVD method using as a template a commercial nickel foam produced by Gelon LIB Group (number of pores per inch: 110 PPI, density e” 250 g·m^{-2}, thickness d” 2.5 mm). First, the nickel foam was cleaned in sonication bath with acetone and isopropyl alcohol, dried and then annealed using a furnace (model EasyTube 2000 produced by CVD Equipment Corporation USA) heated at 1000°C for 15 minutes. Subsequently, 3D graphene was grown on Ni foam using in the same furnace heated at 1000°C a gas mixture of methane (purity > 99.9995%) as carbon source, argon (purity > 99.999%),

---

* *email: cristina.banciu@icpe-ca.ro; Phone: +40 21 3467231*

and hydrogen (purity > 99.995%) and at atmospheric pressure for 60 min. The corresponding flow rates were $3.33{\cdot}10^{-6}$ $m^3{\cdot}s^{-1}$ CH_4, $1.67{\cdot}10^{-5}$ $m^3{\cdot}s^{-1}$ Ar, and $5.42{\cdot}10^{-6}$ $m^3{\cdot}s^{-1}$ H_2. Finally, the graphene sample was rapidly cooled to room temperature under the Ar and H_2 protection [30].

The ZnO nanoparticles were prepared on 3D graphene substrates by hydrothermal process, using a solution containing zinc chloride $ZnCl_2$ (as Zn precursor) and ammonium hydroxide (NH_4OH).

For the hydrothermal process, 2.04 g $ZnCl_2$ were dissolved in 120 mL of deionized water and after this in the solution was added 6 mL 25% NH_4OH solution. 3D graphene substrates and the obtained solution were added in a stainless steel autoclave with 200 mL volume and it was heated in an electric oven at 90°C and 120°C for different times (1.5 h, 2.5 h and 3.5 h). Finally, hybrid ZnO/3D graphene structure was washed with deionized water, it was dried by blowing nitrogen and it was placed in a vacuum oven at 25°C for 24 h for advanced drying.

In order to characterize the morphology and structure of the composite and its intermediate components, the scanning electron microscopy and X-ray diffraction were used. The surface morphology was examined by employing a scanning electron microscope (FESEM, Carl Zeiss Auriga) at an accelerating voltage of 2.00 kV. XRD measurements were performed using a D8 Advance diffractometer at 40 kV voltage and 40 mA current, with Cu/Kα radiation (λ=0.15406 nm). The 2θ angles were set from 25 to 60° with a scanning rate of 2°/min, using grazing incidence method.

Results and discussions

Figure 1 shows comparatively SEM images of nickel foam and 3D graphene deposited on nickel foam, both as intermediate components of the composite. It can be observed that the nickel foam is fully covered with layers of specific structure of graphene, at a growing time of 60 min.

The obtained intermediate sample of 3D graphene was also characterized by X-ray diffraction (fig. 2) and by scanning electron microscopy (fig. 1b). From the diffraction patterns, we can observe the Ni peaks situated at 44.8°, 52.2° and 76.9°, and the carbon peak situated at 26.75°. The intensity of the carbon diffraction peak is much lower than that of the nickel diffraction peaks because the nickel foam is covered by a thin multi-layer graphene, as confirmed by Raman analysis [30].

Hydrothermal synthesis of 1D ZnO structures from $ZnCl_2$-NH_4OH aqueous system has been carried out successfully in the last years. However, due to the ZnO various morphologies, the growing mechanism of the hydrothermal process still needs further study in order to be fully understood. Zinc (II) cation and ammonia combined in solution form the complex ion (tetra-ammonium zincate ion), $Zn(NH_3)_4^{2+}$. We can propose a mechanism of growing process of ZnO crystallites by the following chemical reactions (which are in concordance with the obtaining of ZnO nanorods [31]):

$$NH_3 + H_2O \text{ « } NH_3 \times H_2O \leftrightarrow NH_4^+ + OH^- \quad (1)$$

$$Zn^{2+} + 4\,NH_3 \leftrightarrow [Zn(NH_3)_4]^{2+} \quad (2)$$

$$[Zn(NH_3)_4]^{2+} + 4\,OH^- \leftrightarrow ZnO_2^{2-} + 2\,H_2O + 4\,NH_3 \quad (3)$$

$$ZnO_2^{2-} + H_2O \leftrightarrow ZnO + 2\,OH^- \quad (4)$$

As the proposed reactions (3) and (4) indicate, the transformation in alkaline medium of $[Zn(NH_3)_4]^{2+}$ cation into ZnO may be incomplete, leading to a possible intermediate phase of $Zn(OH)_2$. However, the $Zn(OH)_2$ phase was not detected by XRD. This suggests that either $Zn(OH)_2$ exists inside the layer only as an amorphous phase or it was transformed to ZnO at our working temperatures (90°C and 120°C) which exceed 50°C, as Gao and coworkers have suggested [32, 33].

The process of ZnO growing on the 3D graphene substrate by hydrothermal method can be explained, in agreement with the scientific literature [34]. The authors of this reference supposed a chemical reaction where the zinc cation is coupled with graphene oxide in the presence of alkaline medium, leading to a $(GOZn)^{z+}zOH^-$ neutral complex. Then, this complex can react with the $Zn(OH)_4^{2-}$ soluble species and therefore the ZnO solid compound can occur both as G(ZnO) retained particles on graphene structure and as ZnO free particles.

Influence of temperature growing

To study the influence of the temperature on the properties of 1D ZnO nanoparticles grown on 3D graphene

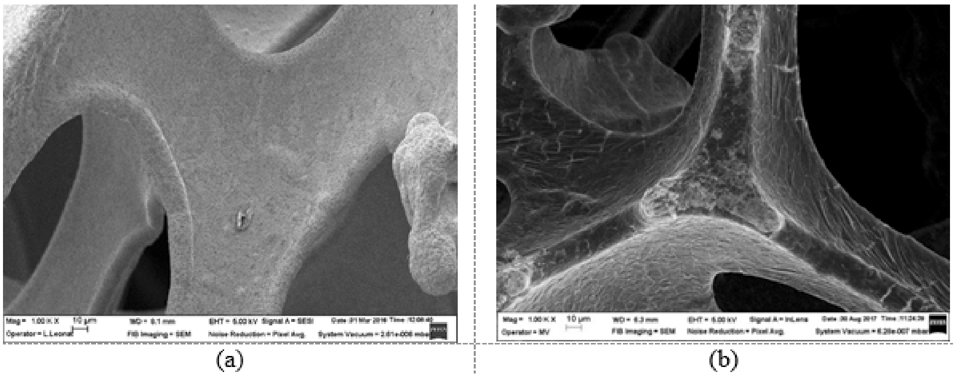
(a)

(b)

Fig. 1. SEM images of nickel foam (a) and 3D graphene structure obtained on nickel foam (b)

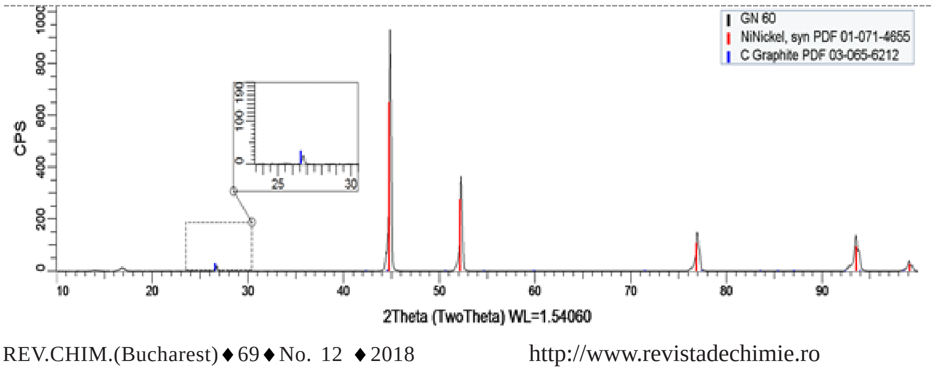

Fig. 2. XRD pattern for 3D graphene structure obtained on nickel foam

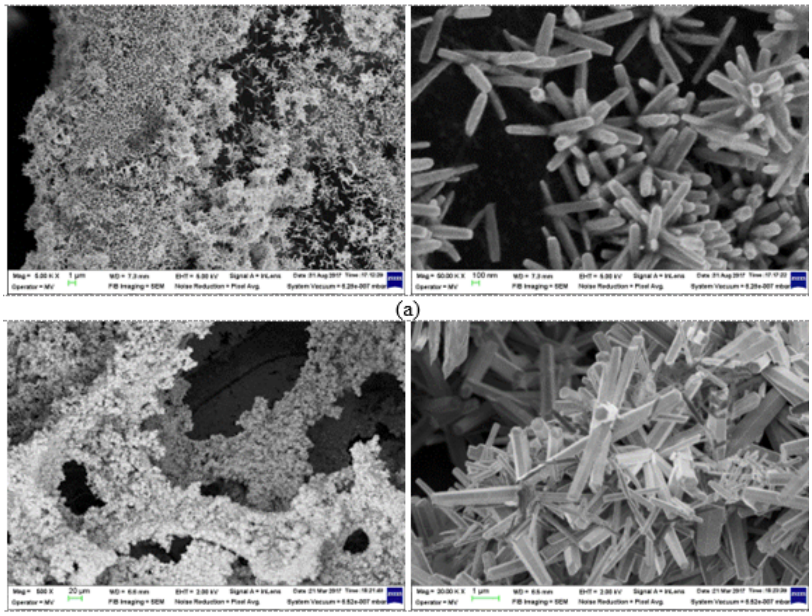

Fig. 3. SEM images of ZnO nanoparticles grown on 3D graphene substrate at 90°C (a) and 120°C (b) for 1.5 h hydrothermal process

structure, we used the same parameters for the hydrothermal process: solution system $ZnCl_2$ and NH_4OH, reaction time 1.5 h, and the dimensions of the 3D graphene substrate. The only variable of the process was the temperature, which varied between 90°C and 120°C. The obtained samples with ZnO/3D graphene hybrid structure samples were structurally characterized by X-ray diffraction and by scanning electronic microscopy.

In the case of the prepared hybrid ZnO/3D graphene structure at a low temperature of 90°C (fig. 3a), we can see that ZnO nanoparticles were obtained, but these are not homogeneously oriented and distributed on the entire surface of the 3D graphene substrate. By increasing the temperature up to 120°C, ZnO nanoparticles fully covered the 3D graphene substrate. From the morphological characterization, we can conclude that the nanoparticles dimensions and the shape are strongly influenced by the temperature of the hydrothermal process. By increasing the temperature from 90 to 120°C, the length of the nanoparticles increased from 550 nm to 2100 nm and their diameters increased from 150 nm to 500 nm.

The XRD patterns show that despite the nickel peaks that appears from the substrate, all the other diffraction peaks confirm that zinc oxide has a hexagonal crystalline structure of wurtzite. The high intensities of the diffraction peaks suggest that it was more crystalline at a synthesis temperature of 120°C (fig. 4b) than at 90°C (fig. 4a).

The influence of growing time

In the case of growing time variation, the hydrothermal process for 1D ZnO particle obtaining on 3D graphene substrate was carried out for 1.5 h, 2.5 h and for 3.5 h at 90°C. The SEM results are shiown in figure 5. From the images, we can observe that for the shortest growing time of 1.5 h (fig. 5a), ZnO nanoparticles were obtained, but these did not fully cover the 3D graphene substrate. By increasing the growing time to 2.5 h (fig. 5b), the substrate was completely covered and the nanoparticle size increased. If the growing time increases up to 3.5 h (fig.

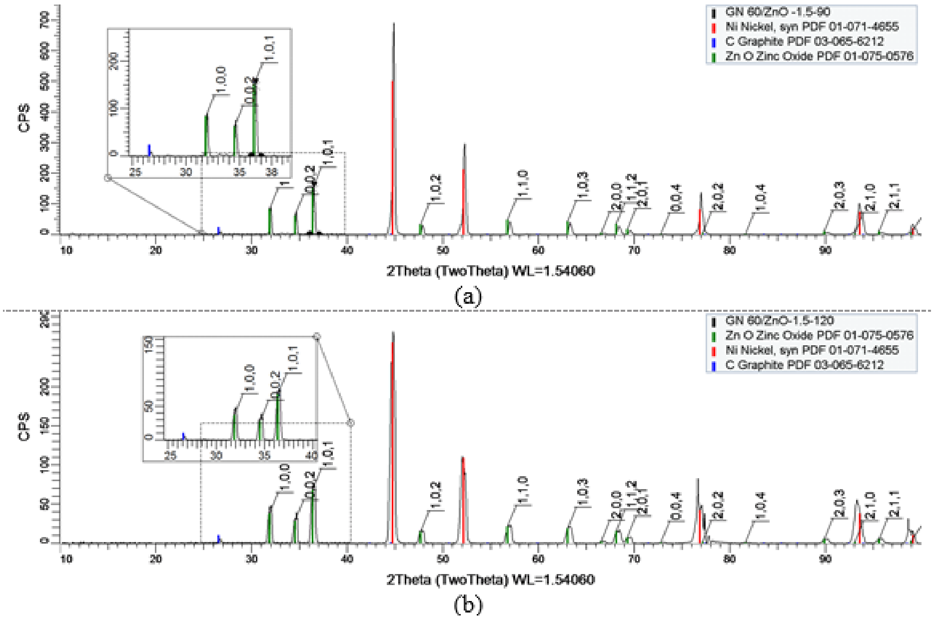

Fig. 4. XRD patterns of ZnO nanoparticles obtained by hydrothermal growth at 90°C (a) and 120°C (b) for 1.5 h

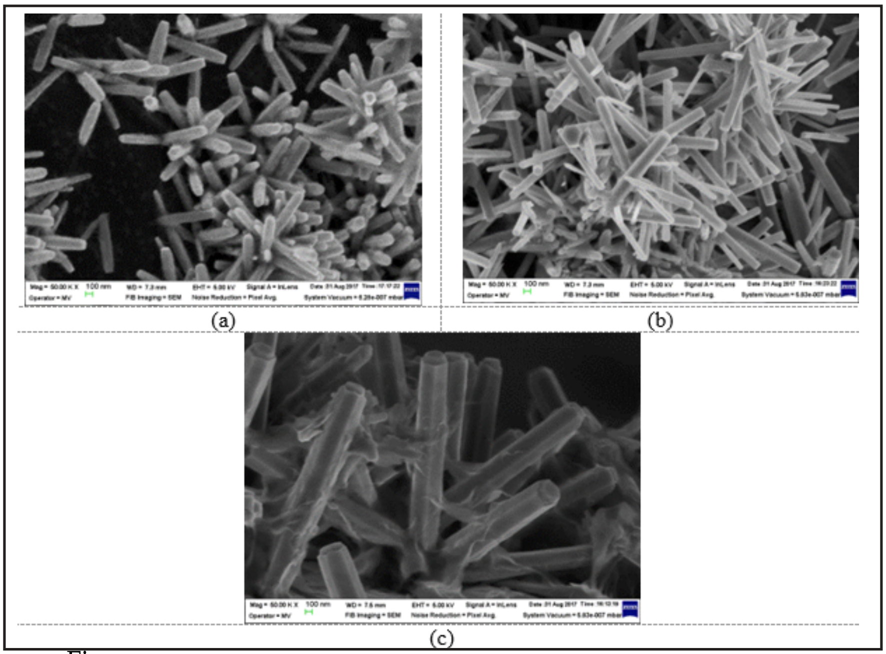

Fig. 5. SEM images for ZnO nanoparticle hydrothermally grown for 1.5 h (a), 2.5 h (b) and 3.5 h (c) at 90°C

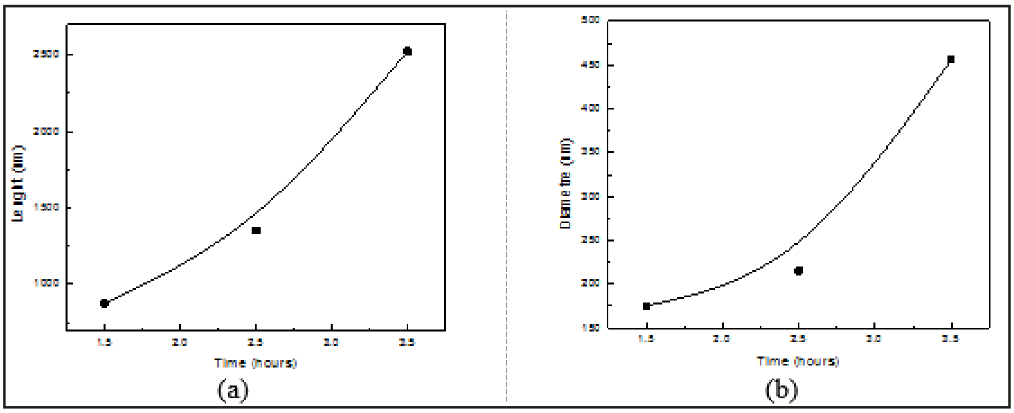

Fig. 6. The length (a) and diameter (b) of the ZnO nanoparticles hydrothermally grown at different times.

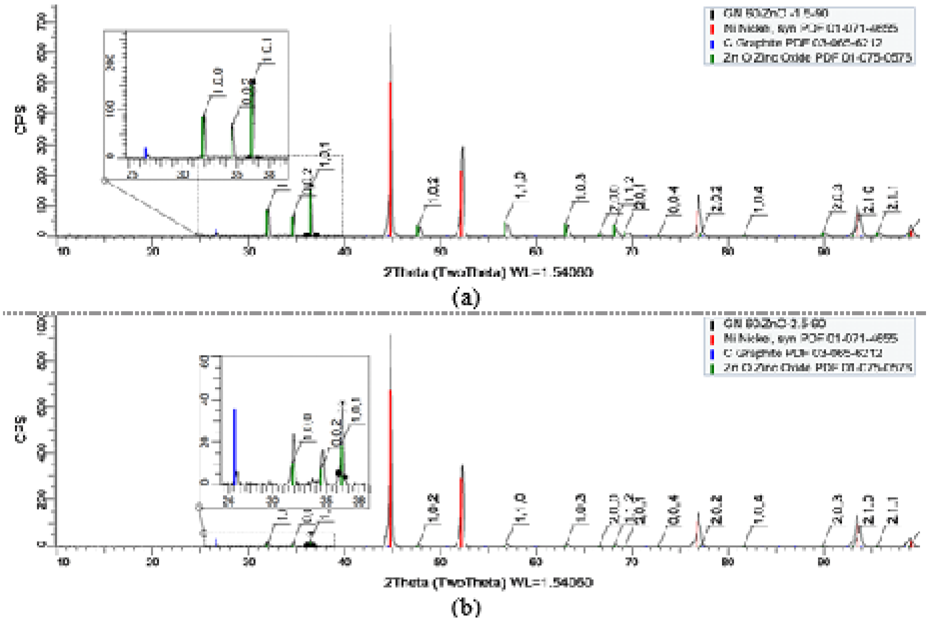

Fig. 7ab. XRD patterns of the ZnO nanoparticles hydrothermally grown for 1.5 h (a), 2.5 h (b)

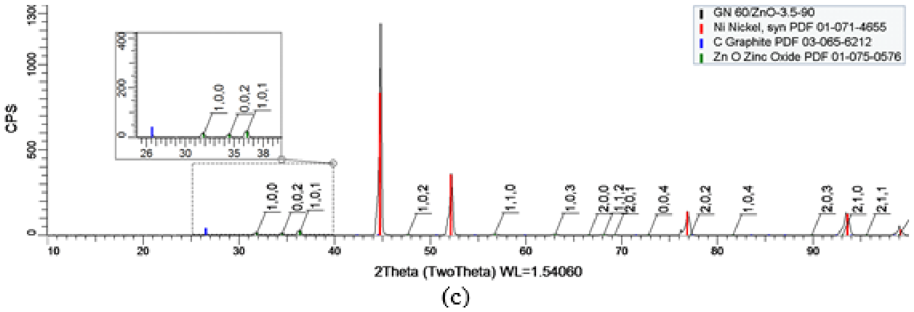

Fig. 7c. XRD patterns of the ZnO nanoparticles hydrothermally grown for 3.5 h

5c), ZnO particles with the largest dimensions, micrometer sizes, were obtained.

Thus, by increasing the growing time, the dimensions of 1D ZnO particles increased in length and diameter (figs. 6a and 6b) from 550 nm/150 nm at a growing time of 1.5 h, to 1200 nm/200 nm for 2.5 h and reaching 2500 nm/480 nm for 3.5 h.

The ZnO/3D graphene hybrid structures were also characterized by the XRD technique and the results are shown in figure 7. It can be seen that three diffraction peaks appear on the patterns at 2θ = 31.7°, 34.3°, and 36.2°, indexed as (1 0 0), (0 0 2), (1 0 1) orientation planes, respectively, and they represent the specific peaks for hexagonal phase of wurtzite crystalline structure. The peaks are more intense at 2.5 h (fig. 7b) and 1.5 h (fig. 7a) deposition times. By increasing the growing time to 3.5 h (fig. 7c), the structure became more amorphous, and only the Ni substrate can be seen in the XRD pattern. With the exception of ZnO and Ni phases, no characteristic peaks of impurities phases were found, which revealed a good crystallinity.

Conclusions

In our study hybrid ZnO/3D graphene structures were successfully obtained by using a complex process that implies the hydrothermal growing of 1D ZnO nanoparticles on a substrate of 3D graphene prepared previously by chemical vapour deposition on nickel foam.

The growing temperature had a strong influence during the hydrothermal process for preparation of 1D ZnO nanoparticles, regarding both size and density of the particles grown on the substrate. By increasing the temperature of the hydrothermal process from 90°C to 120°C, ZnO nanoparticles covered all 3D graphene substrate and the particle sizes increased almost 4 times.

The growing time also has an influence of the structural and morphological properties of the 1D ZnO nanoparticles, the best samples being prepared at process time duration of 2.5 h.

By controlling the parameters of hydrothermally process, the structural and morphological properties of the 1D ZnO nanoparticles can be tailored.

Acknowledgement: This work was supported by a grant of the Romanian National Authority for Scientific Research and Innovation, CNCS – UEFISCDI, project number - PN-III-P2-2.1-PED-2016-1159 (129PED/2017) and the Bilateral Collaboration Romania-Russia, project position 39 from the JINR Order no. 322/21.05.2018 Obtaining and characterization of 3D graphene/ZnO composite networks.

References

1. YANG, P.K., CHANG, W.Y., TENG, P.Y., JEN, S.F., LI, S.J., CHIU, P.W., HE, J.H., Proc. IEEE, **101**, 2013, p. 1732.
2. TSAI, D.S., LIU, K.K., LIEN, D.H., TSAI, M.L., KANG, C.K., LIN, C.A., LI, L.J., HE, J.H., ACS Nano, **7**, 2013, p. 3905.
3. FIGUEIREDO-FILHO, L.C.S., BROWNSON, D.A.C., FATIBELLO-FILHO, O., BANKS, C.E., Electroanalysis, **26**, no. 1, 2014, p. 93.
4. CHEN, Z., XU, C., MA, C., REN, W., CHENG, H.M., Adv. Mater., **25**, no. 9, 2013, p. 1296.
5. DONG, X., CAO, Y., WANG, J., CHAN-PARK, M.B., WANG, L., HUANG, W., CHEN, P., RSC Adv., **2**, 2012, p. 4364.
6. SHERRELL, P.C., MATTEVI, C., Materials Today, **19**, no. 8, 2016, p. 428.
7. LI, X.S., CAI, W.W., AN, J.H., KIM, S., NAH, J., YANG, D.X., PINER, R., VELAMAKANNI, A., JUNG, I., TUTUC, E., BANERJEE, S.K., COLOMBO, L., RUOFF, R.S., Science, **324**, 2009, p. 1312.
8. GULDI, D.M., SGOBBA, V., Chem. Commun., **47**, 2011, p. 606.
9. MAUTER, M.S., ELIMELECH, M., Environ. Sci. Tech., **42**, 2008, p. 5843.
10. BRENNAN, L.J., BYRNE, M.T., BARI, M., GUNKO, Y.K., Adv. Energy Mater., **1**, 2011, p. 472.
11. TSAI, T.H., CHIOU, S.C., CHEN, S.M., Int. J. Electrochem. Sci., **6**, 2011, p. 3333.
12. CHANG, W.-C., CHENG, Y.-Y., YU, W.-C., YAO, Y.-C., LEE, C.-H., KO, H.-H., Nanoscale Res. Lett., **7**, 2012, p. 166.
13. RAMAR, A., SOUNDAPPAN, T., CHEN, S.-M., RAJKUMAR, M., RAMIAH, S., Int. J. Electrochem. Sci., **7**, 2012, p. 11734.
14. CHAI, G., LUPAN, O., CHOW, L., HEINRICH, H., Sens. Actuat. A Phys., **9**, 2009, p. 184.
15. PREPELITA, P., CRACIUN, V., SBARCEA, G., GAROI, F., Appl. Surf. Sci., **306**, 2014, p. 47.
16. PARK, W.I., KIM, D.H., JUNG, S.W., YI, G.C., Appl. Phys. Lett., **9**, 2002, p. 4232.
17. BAKIN, A., MOFOR, A.C., EL-SHAER, A., WAAG, A., Superlattice Microst., **9**, 2007, p. 33.
18. SUH, D.I., BYEON, C.C., LEE, C.L., Appl. Surf. Sci., **9**, 2010, p. 1454.
19. FULATI, S., ALI, M.U., ASIF, M.H., ALVI, N.H., WILLANDER, M., BRÄNNMARK, C., BÖRJESSON, S.I., ELINDER, F., DANIELSSON, B., Sensor Actuat. B Chem., **9**, 2010, p. 673.
20. CHITANU, E., DANESCU-PISLARU, L., EL-LEATHEY, A.L., CHIHAIA, R., BABUTANU, C., MARINESCU, V., SBARCEA, G.B., Proc. IEEE, 10th International Symposium on Advanced Topics in Electrical Engineering ATEE, 2017, p. 768.
21. GONZALEZ-VALLS, I., LIRA-CANTU, M., Energy Environ. Sci., **2**, 2009, p. 19.
22. WU, J.S., XUE, D.F., Sci. Adv. Mater., **3**, 2011, p. 127.
23. SUCHEA, M., TUDOSE, I.V., IONITA, S., SANDU, I., IACOMI, F., KOUDOUMAS, E., Rev. Chim. (Bucharest), **66**, no. 12, 2015, p. 2044.
24. VAJA (DUMITRU), F., COMANESCU, C., OPREA, O., FICAI, D., GURAN, C., Rev. Chim. (Bucharest), **63**, no. 7, 2012, p. 722.
25. HU, X.B., ZHANG, H.J., NI, Y.W., ZHANG, Q., CHEN, J.P., Biosens. Bioelectron., **24**, 2008, p. 93.
26. ZHANG, Q., DANDENEAU, C.S., ZHOU, X., CAO, G., Adv. Mater., **21**, 2009, p. 1.
27. XU, F., SUN, L., Energy Environ. Sci., **4**, 2011, p. 818.

28. EFFENDI, N.A.S., SAMSI, N.S., ZAWAWI, S.A., HASSAN, O.H., ZAKARIA, R., YAHYA, M.Z.A., ALI, A.M.M., AIP Conference Proceedings, **1877**, 2017, Article 090005, DOI: 10.1063/1.4999900.

29. VECA, L.M., NASTASE, F., BANCIU, C., POPESCU, M., ROMANITAN, C., LUNGULESCU, M., POPA, R., Diam. Relat. Mater., **87**, 2018, p. 70.

30. BANCIU, C., LUNGULESCU, M., BARA, A., LEONAT, L., TEISANU, A., Optoelectron. Adv. Mat. - Rapid Commun., **11**, no. 5-6, 2017, p. 368.

31. SUN, X.M., CHEN, X., DENG, Z.X., LI, Y.D., Mater. Chem. Phys., **78**, 2003, p. 99.

32. GAO, X.D., LI, X.M., YU, W.D., LI, L., PENG, F., ZHANG, C.Y., J. Cryst. Growth 291, no. 1, 2006, p. 175.

33. RAKHSHANI, A.E., KOKAJ, J., MATHEW, J., PERADEEP, B., Appl. Phys. A, **86**, 2007, p. 377.

34. LIU, S., SUN, H., SUVOROVA, A., WANG, S., Chem. Eng. J., **229**, 2013, p. 533.

Manuscript received: 16.03.2018